X-Ray Bragg Diffraction in Asymmetric Backscattering Geometry

Yu. V. Shvyd'ko*
Advanced Photon Source, Argonne National Laboratory, Argonne, Illinois 60439, USA

M. Lerche
University of Illinois at Urbana-Champaign, Urbana, Illinois 61801, USA
Advanced Photon Source, Argonne National Laboratory, Argonne, Illinois 60439, USA

U. Kuetgens
Physikalisch-Technische Bundesanstalt (PTB), Braunschweig, D-38116 Germany

H. D. Rüter
Institut für Experimentalphysik, Universität Hamburg, D-22761 Germany

A. Alatas and J. Zhao
Advanced Photon Source, Argonne National Laboratory, Argonne, Illinois 60439, USA
(Received 9 May 2006; published 8 December 2006)

We observe three effects in the Bragg diffraction of x rays in backscattering geometry from asymmetrically cut crystals. First, exact Bragg backscattering takes place not at normal incidence to the reflecting atomic planes. Second, a well-collimated ($\simeq 1$ μrad) beam is transformed after the Bragg reflection into a strongly divergent beam (230 μrad) with reflection angle dependent on x-ray wavelength—an effect of angular dispersion. The asymmetrically cut crystal thus behaves like an optical prism, dispersing an incident collimated polychromatic beam. The dispersion rate is $\simeq 8.5$ mrad/eV. Third, parasitic Bragg reflections accompanying Bragg backreflection are suppressed. These effects offer a radically new means for monochromatization of x rays not limited by the intrinsic width of the Bragg reflection.

DOI: 10.1103/PhysRevLett.97.235502 PACS numbers: 61.10.−i, 41.50.+h, 42.25.Fx

Do optical prisms dispersing visible light and single crystals diffracting x rays share anything in common?

Almost 100 years after discovery and extensive and accurate studies, covered in a great number of publications, little remains unknown and unobserved related to Bragg diffraction of x rays. However, unexplored areas concealing a wealth of new knowledge still exist even in such a very well-charted terrain. Such a surprisingly untried area, opening new physical effects and perspectives of applications, is Bragg diffraction in backscattering from asymmetrically cut perfect crystals. As we demonstrate in this Letter, such crystals behave, in particular, like optical prisms, dispersing collimated polychromatic light. The dispersion rate is $\simeq 8.5$ mrad/eV, almost as big as for visible light in a prism. This may seem to be a paradox, since the effect of refraction for x rays is many orders of magnitude smaller. Similar to optical prism, Bragg backscattering from asymmetrically cut crystals offers a variety of applications.

Sets of parallel atomic planes in crystals can totally reflect x rays provided the glancing angle of incidence θ to the planes and the x-ray photon energy E are related by Bragg's law $2d_H \sin\theta = \lambda(1 + w_H^{(s)})$, where $\lambda = hc/E$ is the wavelength of the x rays in vacuum, d_H is the spacing between the atomic planes, corresponding to the reciprocal vector $\boldsymbol{H}$, and $w_H^{(s)}$ is a refractive correction. The dynamical theory of Bragg diffraction in perfect crystals (for details and references to original publications, see, e.g., recently published books on x-ray diffraction [1,2]) predicts that total reflection of x rays is actually achieved in a small range of photon energies $\Delta E^{(s)} = \epsilon_H^{(s)} E$, and glancing angles of incidence $\Delta\theta^{(s)} = \epsilon_H^{(s)} \tan\theta$ around the values of θ and E determined by Bragg's law. For a given Bragg reflection, the refractive correction $w_H^{(s)}$ and the relative spectral width $\epsilon_H^{(s)}$ are to a good accuracy constants independent of E and θ. They are small, e.g., for the (008) Bragg reflection in Si, which will be considered in the following, $w_{008}^{(s)} = 5.87 \times 10^{-6}$ and $\epsilon_{008}^{(s)} = 2.96 \times 10^{-6}$.

The angular and spectral widths of Bragg reflections change from the values given above, if the crystal surface makes a nonzero angle η, the asymmetry angle, to the diffracting atomic planes, as in Fig. 1. The angular width becomes $\Delta\theta = \Delta\theta^{(s)}/\sqrt{|b|}$, and the energy width $\Delta E = \Delta E^{(s)}/\sqrt{|b|}$. Here, b is the asymmetry parameter, defined as $b = -\sin(\theta \pm \eta)/\sin(\theta \mp \eta)$. The upper sign corresponds to the positive x' component of the wave vector $\boldsymbol{K}_0$ ($|\boldsymbol{K}_0| = 2\pi/\lambda$) of the incident radiation as shown in Fig. 1. If the atomic planes are parallel to the crystal surface, i.e., $\eta = 0$, then $b = -1$, which defines symmetric Bragg diffraction. In all other cases, i.e. $\eta \neq 0$, the corresponding Bragg diffraction is asymmetric. By choosing a proper b, one can tailor the widths of Bragg reflections to better suit certain applications. This technique is in

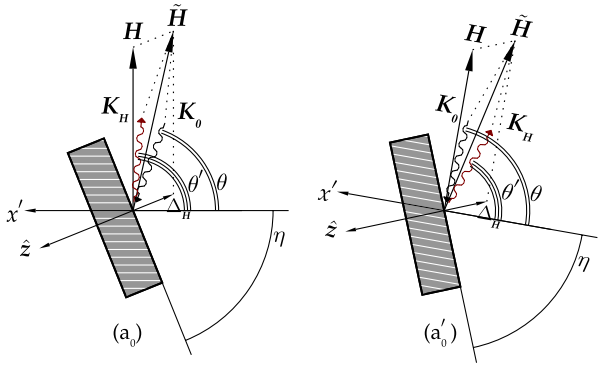

FIG. 1 (color online). Schematic drawing illustrating Bragg diffraction in the asymmetric backscattering geometry, with the asymmetry angle $\eta \neq 0$. Exact backscattering ($\theta = \theta'$) is attained in the transition from (a) to (b) while increasing θ.

use in x-ray optics. In particular, it allows one to build x-ray monochromators with very high energy resolution; see [2–4] for more details and references.

However, in backscattering geometry, i.e., when $\theta \to \pi/2$, the asymmetry parameter is $b \simeq -1$ independent of η. As a consequence, the Bragg reflection widths are unaffected by the asymmetry. This fact usually leads to the general conclusion that there is no or only an insignificant effect of the crystal asymmetry on Bragg diffraction in backscattering [5]. The asymmetry parameter indeed becomes independent of η, with $b = -1$ in backscattering. This does not imply, however, that there are no effects of the asymmetry. This implies merely that b is no longer a representative parameter of the problem. The effects still exist, but in different forms [2] that will be demonstrated in this Letter.

The effects of the crystal asymmetry have one origin—refraction at the vacuum-crystal interface. The total momentum transfer $\tilde{\boldsymbol{H}} = \boldsymbol{K}_H - \boldsymbol{K}_0$ in scattering from a crystal of an incident wave with wave vector $\boldsymbol{K}_0$ into a wave with vacuum wave vector $\boldsymbol{K}_H$ ($|\boldsymbol{K}_H| = |\boldsymbol{K}_0|$) is given not only by the diffraction vector $\boldsymbol{H}$ but also by a small yet important additional momentum transfer $\boldsymbol{\Delta}_H = \Delta_H \hat{\boldsymbol{z}}$ due to scattering at the interface, i.e., $\tilde{\boldsymbol{H}} = \boldsymbol{H} + \boldsymbol{\Delta}_H$ (see Fig. 1). Compared to H, $|\Delta_H|$ is of the order of magnitude of $w_H^{(s)}$. $\boldsymbol{\Delta}_H$ is antiparallel to the internal surface normal $\hat{\boldsymbol{z}}$. If $\eta = 0$ then $\tilde{\boldsymbol{H}}$ and $\boldsymbol{H}$ are parallel, and the glancing angles of incidence θ and reflection θ' are always equal. This is illustrated in Fig. 2(b), which shows the region of total Bragg reflection in the phase space of incident (λ, θ) and reflected (λ, θ') waves, close to normal incidence when $\theta \to \pi/2$. However, if $\eta \neq 0$ then $\tilde{\boldsymbol{H}}$ and $\boldsymbol{H}$ are not parallel, as in Fig. 1, and the glancing angles of incidence θ and reflection θ' are not equal in all cases except for one, when $\boldsymbol{K}_H = -\boldsymbol{K}_0$, i.e., in *exact* backscattering. However, unlike the symmetric case, now exact backscattering cannot take place at normal incidence to the reflecting atomic planes, i.e., when $\theta = \pi/2$, as can be seen from Figs. 1(a) and 1(b) . It takes place at

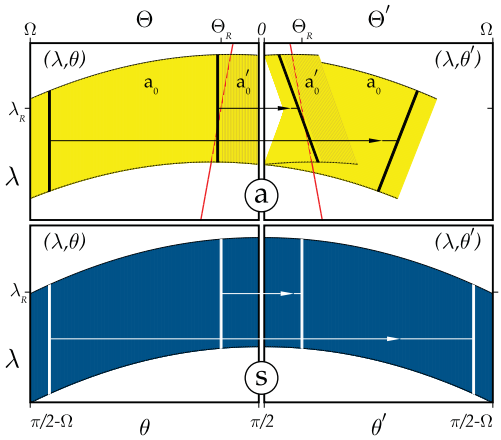

FIG. 2 (color). Transformation of the Bragg reflection region from the (λ, θ) space of incident waves in the vicinity of normal incidence, into the (λ, θ') space of exit waves. (s) Symmetrically cut crystal: $\eta = 0$. (a) Asymmetrically cut crystal: $\eta \neq 0$. The red line is a locus of points obeying exact backscattering condition in asymmetric scattering geometry, given by Eq. (3). It is a borderline between scattering geometries of Figs. 1(a) and 1(b). $\Omega = 0.1^\circ = 1.7$ mrad.

$$\theta_R = \pi/2 - \Theta_R, \qquad \Theta_R = w_H^{(s)} \tan\eta. \tag{1}$$

Here Θ_R is the incidence angle of exact backscattering for x rays with wavelength $\lambda = \lambda_R \simeq 2d_H(1 - w_H^{(s)})$ at the center of the spectral region of total reflection. One should not, however, mistake this effect for the refraction correction to the Bragg angle.

More importantly, the additional momentum transfer Δ_H depends on the radiation wavelength (photon energy). This means that the reflection angle θ' varies with wavelength, even if the glancing angle of incidence is constant. The variation is given by

$$\delta\theta' = (\delta\lambda/\lambda)(1 + b)\tan\theta.$$

Asymmetrically cut crystals behave like optical prisms, dispersing a collimated incident polychromatic beam. One may think, however, that this effect vanishes in backscattering, because in this case $(b + 1) \to 0$. On the contrary, since $\tan\theta$ becomes large, the effect increases. In backscattering, it is expressed by another equation:

$$\delta\theta' = -\delta\Theta' = 2\frac{\delta\lambda}{2d_H}\tan\eta. \tag{2}$$

Both results, presented by Eqs. (1) and (2) were predicted in [2]. The second effect was termed angular dispersion.

Both effects are illustrated in Fig. 2(a). The marked areas show the region of total reflection in the phase space of incident (λ, θ) and reflected (λ, θ') waves. A detailed explanation of how an asymmetric Bragg reflection changes the DuMond diagram for the exit beam is given in [2]. Unlike the $\eta = 0$ case shown in Fig. 2(b), they are no longer symmetric. The bold vertical lines in (λ, θ) indicate particular cases of incident beams comprising different wavelengths with the same angle of incidence.

The inclined bold lines in (λ, θ') show the response of the crystal, thus demonstrating the effect of angular dispersion.

The effect of angular dispersion requires that the angles of incidence and reflection for exact backscattering change with the wavelength: the larger the glancing angle of incidence $\Theta = \pi/2 - \theta$ the smaller the wavelength of x rays, which can be reflected backwards. Using Eqs. (1) and (2), the relation for exact backscattering reads:

$$\Theta - \Theta_R = \Theta' - \Theta_R = -\frac{\lambda - \lambda_R}{2d_H} \tan\eta. \qquad (3)$$

This is shown graphically by red lines in Fig. 2(a) [2,5].

The scheme of the experimental setup for studying exact Bragg backscattering of x rays from an asymmetrically cut single crystal is shown in Fig. 3. The experiment was performed at beam line 3ID at the Advanced Photon Source. We used the (008) Bragg backreflection from a Si crystal—(D), and x rays with a photon energy $E = 9.1315$ keV. We have chosen the Si(008) due to practical considerations (see [6] for more technical details of the experiment). Any other Bragg reflection could have been used to demonstrate the effects on which we are reporting. The crystal is 175 mm long, with the front face surface cut at the asymmetry angle $\eta = 88.5°$ to the (008) reflecting atomic planes. The side faces of the crystal are almost parallel to the (008) planes. Thus by illuminating the side face or the front face, both symmetric or asymmetric diffraction can be studied.

The x-ray beam incident upon crystal D has a small angular divergence of $\Delta\theta \lesssim 1$ μrad. This is achieved by the (220) Bragg reflection from a Si crystal collimator—(C), cut asymmetrically with the asymmetry angle $\eta_C = 19°$ ($\theta_C = 20.7°$, asymmetry parameter $b_C = -0.05$). Such reflection transforms the primary incident beam with angular divergence of $\simeq 15$ μrad into a beam with b_C-times smaller divergence. Crystal S is cut the same way as C ($\eta_S = \eta_C$). The function of crystal S is to select only those x rays that are reflected exactly backwards from crystal D. The asymmetry parameter in this case is $b_S = 1/b_C = -20$. As a result, only x rays with a reflection angle spread of $\Delta\theta' = \Delta\theta^{(s)}_{220}\sqrt{|b_S|} \simeq 5$ μrad are selected. Here $\Delta\theta^{(s)}_{220} = 23$ μrad is the angular acceptance of the Si(220) symmetric reflection. The (220) atomic planes in crystals S and C are slightly canted to each other by $\psi \simeq 5$ μrad. This ensures that, first, the beam reflected from C is not reflected from crystal S on its way to D. Second, it propagates through crystal S with reduced absorption in anomalous transmission mode [2]. (For the same purpose, crystal S is only 0.2 mm thick.) Third, only those x rays are reflected from crystal S and reach the detector Det, which emanate from crystal D at the glancing angle of reflection $\theta' = \theta - \psi$. Since ψ is very small, we may consider $\theta' = \theta$ to a very good accuracy, i.e., that crystal S selects only those x rays that are reflected exactly backwards.

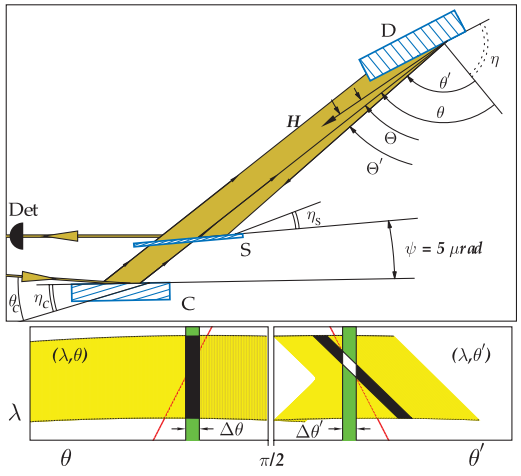

FIG. 3 (color). Top: schematic of the experimental arrangement for studying exact Bragg backscattering of x rays from a single crystal, D. Other components: crystal collimator, C; selector, S; x-ray detector, Det. Bottom: fragment of Fig. 2(a) illustrating operation of the three crystal arrangement.

Figure 4 shows the Bragg reflectivity of crystal D under these conditions as a function of the angle of incidence $\Theta = \pi/2 - \theta$. The beam cross section incident upon crystal D is large enough to illuminate simultaneously both the crystal front face and crystal side face, as illustrated in Fig. 3. The sharp peak at $\Theta = 0$ is the reflectivity of the crystal side face in symmetric exact Bragg backscattering mode. A measured width of $\Delta\tilde{\Theta}_s \simeq 5$ μrad is mostly due to the $\Delta\theta' \simeq 5$ μrad angular acceptance of the crystal selector S. No additional broadening is observed, as expected.

The broad peak is the reflectivity of the face side in asymmetric exact Bragg backscattering. The angular shift of $\tilde{\Theta}_R = 227$ μrad of the center of the reflection region evidences that exact backscattering from an asymmetrically cut crystal takes place not at normal incidence to the reflecting atomic planes, i.e., not at $\Theta = 0$ μrad. The measured angular shift is in agreement with the theoretical value $\Theta_R = 224$ μrad, which is obtained from Eq. (1) with $\eta = 88.5°$ and $w^{(s)}_{008} = 5.87 \times 10^{-6}$.

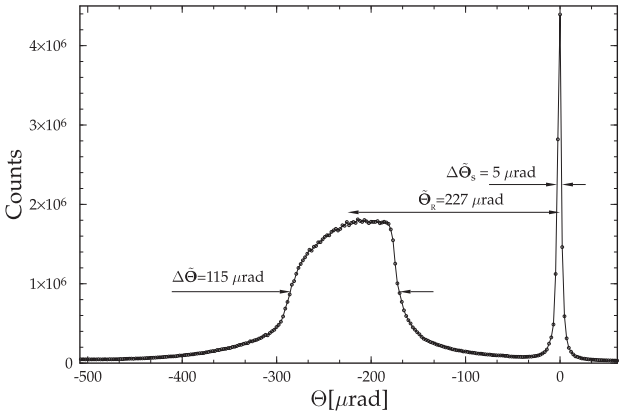

FIG. 4. Bragg reflectivity from crystal D of 9.1315 keV x rays, exactly backwards, as a function of the angle of incidence $\Theta = \pi/2 - \theta$ to the reflecting atomic planes.

The width of the peak demonstrates the magnitude of the effects of angular dispersion. This can be explained with the help of the bottom graph of Fig. 3. The x rays incident upon crystal D are presented by the vertical strip of a width $\Delta\theta \lesssim 1$ μrad in the (λ, θ) phase space. X rays that are reflected are shown in black. In the phase space of reflected x rays (λ, θ'), this region becomes inclined, due to the effect of angular dispersion. The crystal selector S, can reflect only those x rays which are marked by the vertical green line of the angular width $\Delta\theta' = 5$ μrad. Therefore, only those x rays emanating from crystal D are picked up, which fall into the white rhomboid. By changing the angle of incidence, Θ, this white rhomboid moves along the red line, given by Eq. (3) for exact backscattering. Given that the total relative spectral width of the Si(008) reflection is $\epsilon_{008}^{(s)} = 2.96 \times 10^{-6}$, from Eq. (3) we obtain $\Delta\Theta = \Delta\Theta' = 113$ μrad for the spread of the angles of incidence and reflection, for which exact Bragg backscattering is achieved. It is in agreement with the measured value $\Delta\tilde{\Theta} = 115$ μrad. The angular spread of the reflection angles Θ' due to angular dispersion is twice as large [because of the factor two difference in the expressions of Eq. (2) and (3) and thus also in the slopes of the red and black lines in (λ, θ') graph of Fig. 3] and therefore equals $2\Delta\tilde{\Theta} = 230$ μrad. The rate of angular dispersion is $\mathcal{D} = 2\Delta\tilde{\Theta}/\Delta E^{(s)} = 8.5$ μrad/meV. Here $\Delta E^{(s)} = \epsilon_{008}^{(s)} E = 27$ meV is the spectral width of the Si(008) Bragg reflection.

This is, however, not all that the experiment tells us about the effects of the crystal asymmetry on Bragg diffraction in backscattering. There is a third effect, which reveals itself not by the presence but by the absence of a certain feature on the broad reflection peak in Fig. 4. It is known that Bragg backscattering is often accompanied by simultaneous excitation of parasitic Bragg reflections, dramatically reducing the crystal reflectivity into the backscattering channel [7–11]. The Si(008) Bragg reflection is accompanied by two conjugate pairs of parasitic reflections with all reflected waves propagating perpendicular to the incident beam. One pair is suppressed by choosing the polarization of the incident radiation to be in the scattering plane. However, the second pair can still be excited and thus cause a reduction of the crystal reflectivity. This is seen usually as a sharp dip in the reflection curve; see, e.g., [10,11]. The broad peak in Fig. 4, representing reflectivity in exact Bragg backscattering, reveals no signature of any reduction of the crystal reflectivity. Bragg backreflection seems to be unaffected by the accompanying reflections. As was shown theoretically in [2], in asymmetric backscattering geometry with η close to 90°, the strength of the backreflection remains intact, while the strength of the accompanying reflections is suppressed. This is exactly what our experiment evidences.

The observed effects offer a new means for monochromatization of x rays. As the (λ, θ') graph of Fig. 3 suggests, crystal S selects a narrow bandwidth part (white rhomboid) from the dispersed beam of x rays (black strip). We can estimate that in our experiment x rays with a bandwidth of $\approx(\Delta\theta' + \Delta\theta)/\mathcal{D} = 0.7$ meV are selected. The effect of monochromatization depends only on the incident beam divergence $\Delta\theta$, angular acceptance of the wavelength selector $\Delta\theta'$, and the rate $\mathcal{D}$ of angular dispersion [2]. Unlike existing techniques of monochromatization [2–4], relying on the spectral width of Bragg backreflections $\Delta E^{(s)}$, or on the width $\Delta E^{(s)}/\sqrt{|b|}$ modified by the crystal asymmetry, the Bragg width $\Delta E^{(s)}$ plays no role in our case. The first results of the experimental studies of an x-ray monochromator based on this principle are presented in [6].

The effect of angular dispersion can be also used to compress x-ray pulses in time, in a way similar to how it is done with chirped laser pulses.

In summary, we observe three effects in Bragg diffraction of x rays in backscattering geometry from asymmetrically cut crystals: exact Bragg backscattering not taking place at normal incidence to the reflecting atomic planes, angular dispersion, and suppression of parasitic Bragg reflections.

The help of Margit Draht, Barbara Lohl, Benno Frensche (Hamburg University), Albert Dettmer, Dieter Schulze, Jens Hauffe (PTB), Kurt Goetze, and Tim Mooney (APS) in preparation of the experiment is gratefully acknowledged. We thank Dr. Ercan Alp (APS) for assistance during the measurements. Support by Dr. Wolfgang Sturhahn (APS) and Dr. Peter Becker (PTB) is greatly appreciated. Use of the Advanced Photon Source was supported by the US Department of Energy, Office of Science, Office of Basic Energy Sciences, under Contract No. W-31-109-ENG-38.

*Email address: shvydko@aps.anl.gov

[1] A. Authier, *Dynamical Theory of X-Ray Diffraction*, IUCr Monographs on Crystallography Vol. 11 (Oxford University Press, New York, 2001).
[2] Yu. Shvyd'ko, *X-Ray Optics: High-Energy-Resolution Applications*, Optical Sciences Vol. 98 (Springer-Verlag, Berlin, 2004).
[3] T. Matsushita and H. Hashizume, in *Handbook on Synchrotron Radiation*, edited by E. E. Koch (North-Holland, Amsterdam, 1983), Vol. 1, pp. 261–314.
[4] T. S. Toellner, Hyperfine Interact. **125**, 3 (2000).
[5] A. Caticha and S. Caticha-Ellis, Phys. Rev. B **25**, 971 (1982).
[6] Y. V. Shvyd'ko, U. Kuetgens, H. D. Rüter, M. Lerche, A. Alatas, and J. Zhao, AIP Conf. Proc. **879**, 737 (2006).
[7] A. Steyerl and K.-A. Steinhauser, Z. Phys. B **34**, 221 (1979).
[8] C. Giles and C. Cusatis, Appl. Phys. Lett. **59**, 641 (1991).
[9] V. G. Kohn, I. V. Kohn, and E. A. Manykin, JETP **89**, 500 (1999).
[10] J. P. Sutter, E. E. Alp, M. Y. Hu, P. L. Lee, H. Sinn, W. Sturhahn, and T. S. Toellner, Phys. Rev. B **63**, 094111 (2001).
[11] M. Lerche and Yu. V. Shvyd'ko, Phys. Rev. B **70**, 134104 (2004).